ISSN: 2583-9292 (ONLINE)
DOI: 10.21917/ijdsml.2025.0177

ENHANCED BREAST CANCER CLASSIFICATION USING GAN-DRIVEN STAIN NORMALIZATION AND GRAPH-BASED TRANSFORMER NETWORKS

S. Shiny, G. Vaishnavi and R. Kavya Lakshmi
Department of Artificial Intelligence and Data Science, Mepco Schlenk Engineering College, India

Abstract

The identification of breast cancer on histopathology images helps pathologists who need precise and reliable computational methods. This research proposes a unique framework that integrates transformer-based categorization, graph-based tissue modeling, federated learning and Generative Adversarial Network (GAN) to improve diagnostic accuracy. To enhance feature consistency by standardizing histopathology images and to reduce inter-laboratory variances, a stain normalization GAN is used. We use SLIC to divide the tissue regions while maintaining cellular interactions and spatial connectivity and display them as a graph. Connectivity- Aware graph transformer uses connectivity-biased self-attention to capture both global and local topological relationships, which is used to process the retrieved graph features. Federated learning allows collaborative learning while protecting sensitive patient data by ensuring privacy-preserving decentralized model training across several institutions. This method improves model robustness and generalization without centralizing data. The experimental assessment on openly accessible breast cancer datasets shows that our suggested framework performs better in terms of accuracy and interoperability than deep learning models. This paper presents a scalable, privacy-preserving, and clinically practical method for automated breast cancer diagnosis integrating transformer-based classification, connective graph representation, and GAN-based stain normalization within a federated learning paradigm.

Keywords:

GAN based Stain Normalization, Federated Learning, Tissue Graph Construction, Connectivity-Aware Graph Transformer, Breast Cancer Classification

1. INTRODUCTION

. Breast cancer is one of the largest health issues in the world today, and it needs to be identified early and effectively and accurately treated to increase patient survival rates. Since it offers vital information on the appearance and characteristics of tissue, the tumor histopathological examination is generally accepted as the gold standard for detecting breast cancer. Manual histological analysis is difficult, time consuming, and subject to observer variability because tissue structures are so complicated. Recent advances in artificial intelligence (AI) led to the development of deep learning-based automated diagnostic systems. And they provide alternatives to breast cancer classification. Despite advances in stain heterogeneity and data sharing, privacy issues with data sharing, are needed to record long-range linkages within tissue structures. The existence of inter-class similarities and intraclass variations are illustrated in the top and bottom row of Fig.1.

This paper proposes a GAN-Federated Learning and Graph transformer architecture for the classification of breast cancer from histological images[1],[2] to overcome these issues. The advised method integrates transformer architecture, graph-based learning, federated learning (FL), and generative adversarial network for feature extraction, tissue representation, privacy-preserving model training, and for stain normalization. This approach ensures improved model generalization, greater classification accuracy, and robustness to staining variations without endangering patient data privacy. In histopathology, staining heterogeneity [3] is a big problem since different staining techniques, imaging setups, and scanner types cause substantial domain shifts that impair model performance. To lessen the effect of stain-induced variability, histopathology images from various medical facilities are aligned using a stain normalization GAN. The proposed method based on GAN learns a join style by adversarial training, ensuring consistent image representation, in difference to conventional stain normalization techniques, where it frequently call for choosing a target template. This improves model generalization across various datasets in addition to feature extraction.

However, instability, mode collapse, and hyperparameter sensitivity are common problems with traditional GAN training. A technique temporal self-distillation regularization technique is implemented to balance the training process and improve convergence that strengthens the model's stain normalization across dispersed datasets and overcomes the problems.

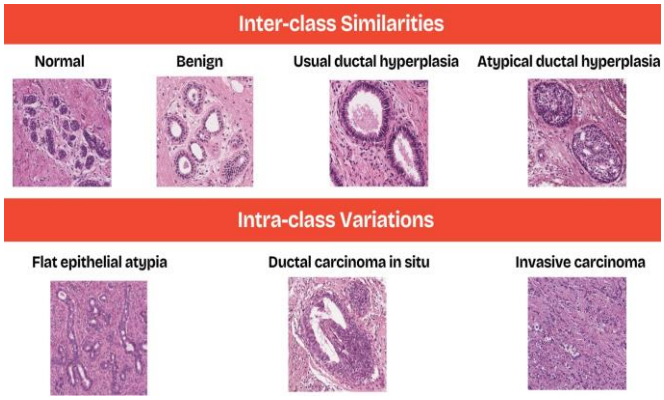

Fig.1. Existence of inter-class similarities and intra-class variations are illustrated in the top and bottom row of Fig.1.

Breast cancer classification has been successful and necessitates accurate modeling of structural arrangements of tissue components in addition to stain normalization. They use a traditional convolutional neural network (CNN) [4] [5] ignoring the spatial relationship between tissue regions that create pixel-based representations. The nodes are used as tissue regions when we create tissue graphs in this research. Through morphological similarities and proximity, lymphocytes, stroma, tumor cells, and edges define spatial interactions. By effectively representing the essential properties of the tissue environment, this graph format provides a biologically relevant feature space for classification.

The structural information from the tissue graph can be fully utilized by using a Connectivity-Aware Graph Transformer. The tissue structures of both short and long-range dependencies are captured by connectivity-aware self-attention mechanism of the advised CGT model, in contrast to the graph neural network (GNN). GNN relies on message passing and only propagates information among neighborhood nodes. A connectivity bias encoding approach is included to highlight spatial interactions between tissue sections during attention calculation and ensure that a closer region contributes more significantly to feature aggregation. To strengthen the ability to distinguish between different subtypes of breast cancer, this method improves the classification performance of the model.

Privacy concerns about the sharing of medical data are now significantly hampered by the development of AI-driven diagnostic models[6]. The pooling of data from various institutions by conventional centralized machine learning institutions presents moral and legal dilemmas about patient privacy. Federated Learning (FL) offered a workable solution that allows several institutions to work together to train a common model without replacing raw patient data. In this project, Fl is integrated into the GAN-Graph transformer framework allowing decentralized learning while preserving data confidentiality. Each institution uses its own private dataset to train a local model; for aggregation, only model changes are sent to a central server. A variety of histopathological data from many sources are used by this method, guaranteeing adherence to data privacy laws.

The efficiency of the suggested approach is demonstrated by performing extensive tests on publicly accessible breast cancer histological datasets. Metrics such as accuracy, precision, recall, F1 score, and AUC-ROC are assessed for classification outcomes. The experimental analysis demonstrates the benefits of combining GAN-based stain normalization, transformerbased feature extraction, graph-based tissue representation, and federated learning, which provides better classification accuracy than the standalone GNN models and the conventional CNN model.

The following are the primary contributions of this work.

- A stain normalization system based on GANs that reduces domain shifts brought on by staining differences and harmonizes histopathology images form various sources.
- Representation of a tissue graph that provides a medically useful feature space by encoding the morphological and spatial interactions between tissue patches.
- A Connectivity-Aware Graph Transfomer (CGT) that captures both short range and long-range interdependence in tissue architectures by combining connectivity bias encoding and self-attention.
- Decentralized collaboration between healthcare facilities without disclosing raw patient data is made possible via a federated learning strategy for the training of model privacy-preserving.
- Comprehensive practical tests on datasets related to breast cancer histology, providing the superiority of the suggested framework over traditional deep learning techniques.

2. RELATED WORK

2.1 STAIN NORMALIZATION IN HISTOPATHOLOGY

The automated breast cancer categorization is the staining variability within histopathological laboratories, which is one of the biggest obstacles. Traditional stain normalization techniques, including color matching [7] methods and stain separation models, have been used frequently to deal with these variances. These techniques have low color mapping and are unable to efficiently extract spatial tissue properties. The capacity to adapt to a variety of datasets is limited in traditional normalizing techniques, since they require preselected template images. So, GAN-based algorithms in deep learning-based stain normalization techniques are proposed beyond these restrictions. Learning the mapping between several staining techniques has helped conditional GANs (cGANs) and cycle-consistent GANs (CycleGANs) [8] demonstrate promising outcomes in stain transfer. All training data are collected in one place, as these models are developed in a centralized environment. Patient data cannot be transferred across institutions, which is limited by their restriction, and they are used in privacy-sensitive medical applications.

Moreover, mode collapse is an issue with traditional GAN based methods in which the generator creates remarkably homogeneous stain patterns that are unable to reflect the range of real histology images. StainGAN had addressed this issue to ensure that morphological tissue structures [9] are

preserved throughout stain normalization by adding further restrictions. The models are unsuitable as they do not account for variations in staining methods throughout institutions for federated learning environments. In this work, a federated GAN-based stain normalization [10] framework is proposed for decentralized staining across several institutions. By including temporal-self-distillation, the proposed method ensures that the generator learns a variety of stain styles from different sources while preserving steady dynamics. This methodology provides a collaborative, privacy-preserving solution for normalizing histopathological images for distant learning contexts.

2.2 FEDERATED LEARNING IN HISTOPATHOLOGICAL IMAGE ANALYSIS

FL is known as a privacy-preserving paradigm [11] [12] which is used to train models together for several institutions without exchanging raw patient data. The model updates are only shared in contrast to traditional centralized learning. FL enables local models to be trained on private datasets that aggregate data from different sources in a single place. This method ensures compliance with laws such as HIPAA and GDPR for medical AI applications. FL [13] has shown comparable performance to centralized training while maintaining data privacy in radiology applications such as brain tumor segmentation and magnetic resonance imaging and COVID-19 identification from chest radiographs. Histopathology is very different from radiography due to normalization [14] of the stain, which is a prerequisite for categorization. Existing FL frameworks do not take into consideration the added computational complexity caused by

stain normalization in histopathology, which is why direct adaption from radiology-based FL models is inefficient.

Differences in tissue morphology, staining, and scanner types result in inconsistent properties of the local data set. The existence of heterogeneous data distributions (non-IID data) in FL-based histopathology presents this difficulty. These variations could lead to the local model diverging, which could reduce the effectiveness of the global model. The influence of current FL methods on stain-normalized histopathology images has not been well investigated, despite their attempts to handle data heterogeneity through strategies like adaptive model aggregation and personalized federated learning. By incorporating stain normalization [15]-[17] directly into the FL pipeline, our work suggests a federated learning approach designed specifically for histopathological image analysis. BY implementing self-distillation-based consistency, the advised approach ensures steady model convergence differences between institutions in staining and imaging procedures. This method makes it possible to use it in a federated medical AI system in the real world and reduces computational overhead.

2.3 HISTOPATHOLOGY: GRAPH-BASED AND TRANSFORMER-BASED LEARNING

The mainstay of traditional deep learning models for histopathological classification is patch-based CNNs. Whole Slide images (WSIs) are divided into smaller fixed-size sections. The spatial interactions between tissue components are not captured, which is essential for the classification [18] of breast cancer. This method makes efficient feature extraction possible. To represent histopathological images, graph-based deep learning is used, which uses networks. In the graph, the edges indicate the spatial and morphological links between them, and the nodes in the graph represent [19], [20] the tissue regions. To perform tasks such as modeling cellular interactions, study of the tumor environment, and categorization of the breast cancer subtype in histopathology, we use graph neural networks (GNNs). Examples of Message-Passing GNNs (MP-GNNs) are Graph convolutional Networks (GCNs) [21] and Graph Attention Networks (GATs) [22] that have shown promise in obtaining significant structural representations from tissue graphs. Node embeddings become indistinguishable due to deep network layers, MP-GNNs suffer from over-smoothing which leads to a loss of discriminative information. Between distant tissue patches, long-distance connections are identified using MP-GNN capacity, and their aggregation is limited to the localized neighborhood.

To describe the local and global feature interactions, transformer-based graph learning models have been proposed and they employ self-attention mechanisms. To employ positional encoding and attention bias to enhance structural awareness in graph-based learning, we use methods such as Graphormer [23],[24] and SAN (Structural Awareness Transformer). Molecular graphs and social network analysis were developed. The main reason is as these are not the best for identifying histopathological images. In this research, the method based on the connectivity-aware graph transformer is presented to classify breast cancer for histopathology images. Existing transformer-based graph models CGT integrate spatial connection bias into self-attention calculations, ensuring that nearby tissue regions make a greater significant contribution to feature aggregation. To distinguish between the characteristics of the tumor, the stromal, and the normal tissue, this method improves the accuracy and interpretability of the model's classification by strengthening its capacity. This work introduces a novel privacy-preserving, scalable, and medically interpretable AI framework that combines GAN-based stain normalization, federated learning, and graph transformer-based classification to diagnose breast cancer using histopathological images.

3. METHODOLOGY

3.1 PROBLEM FORMULATION AND ASSUMPTIONS

The consequence of stain heterogeneity, privacy concerns in data sharing, and the need for robust feature extraction techniques describe different challenges in breast cancer classification in histopathological images. Due to privacy restrictions and institutional policies, deep learning models depend on large, often unavailable, centralized datasets. They proposed a Federated Learning approach (FL)-based learning to address this issue, which allows collaborative model training across multiple institutions without compromising data privacy. GAN is integrated with tissue graph construction and the connectivity-aware graph transformer (CGT) for classification, which is the proposed work. Stain variations arise due to differences in staining protocols, scanner settings, and laboratory conditions between different organizations, which is one of the fundamental challenges in histopathological image analysis. Generalization leads to domain shifts and makes it difficult for deep learning models. We utilized a GAN-based stain normalization [25]technique in a federated learning environment to overcome the problem. This model learns an optimal stain-invariant representation instead of using a fixed stain normalization target. This aggregates knowledge from multiple local discriminators; each of which represents a different institution's staining style. The cancerous and non-cancerous regions reveal complex spatial relationships, where the key challenge is the high-resolution nature of histopathology images. We construct tissue graph instead of dealing with images as a simple grid of pixels where nodes represent distinct tissue regions, and edges capture spatial dependencies between them. This permits the model to diagnose cancer and better encode biological structures. To train both local discriminators for GAN-based stain normalization and tissue graph models, each client (institution) has access to its dataset and computational resources. They donate model updates to the global server since the medical data are highly sensitive, institutions cannot share raw images.

They ensure that privacy is maintained by a decentralized setup while still benefiting from collaborative learning. Due to non-i.i.d. data distributions, federated learning setups often suffer from model divergence. We integrate temporal self distillation to overcome the problem of smoothing parameter updates between multiple training iterations, preventing mode collapse, and improving convergence stability. By incorporating connectivity-aware self-attention mechanisms, classification is performed using CGT and improves the representation of tissue graphs.

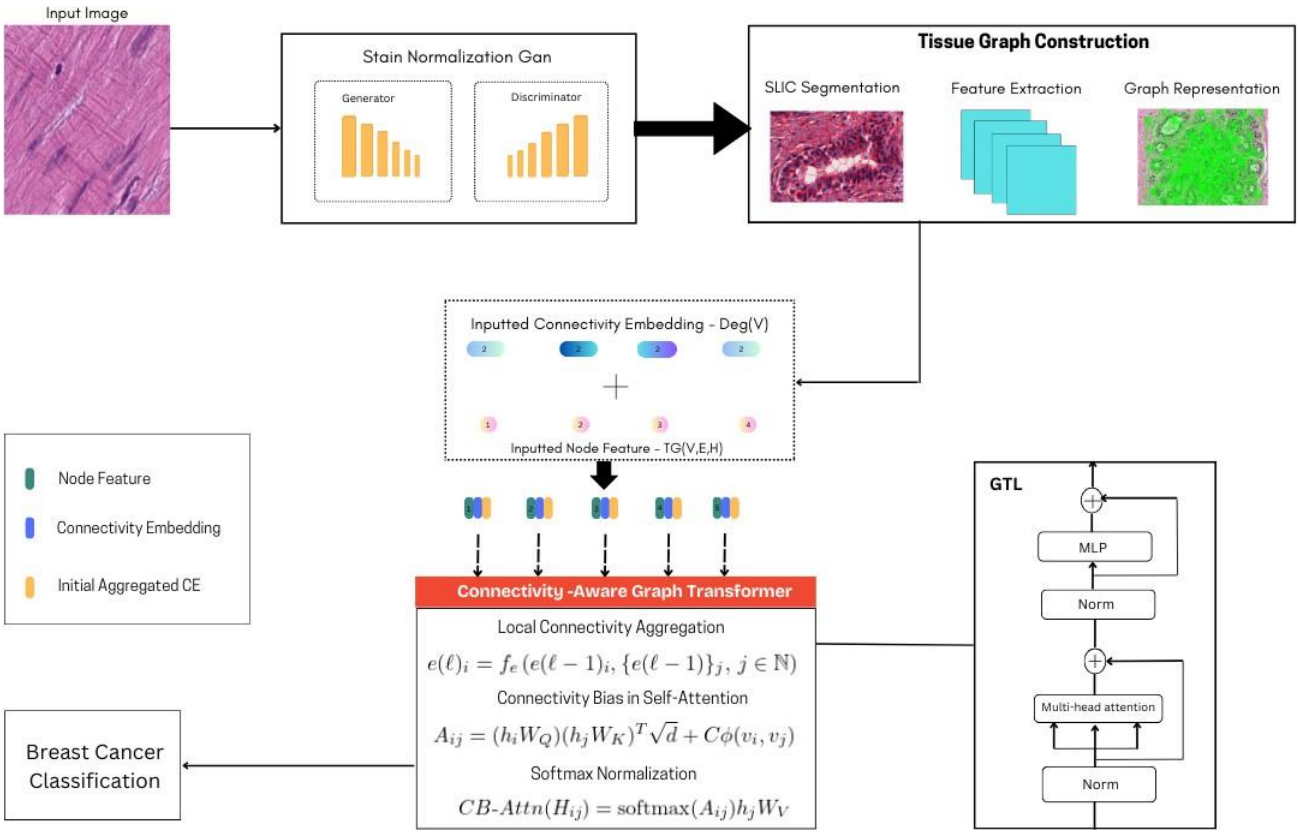

Fig.2. Schematic overview of the proposed framework of Breast Cancer Classification System

3.2 STAIN NORMALIZATION GAN

3.2.1 Generator and Discriminator:

The performance of stain normalization in histopathological images is utilized by the optimized U-Net architecture while preserving the fine-grained morphological structures of the tissues in the generator framework. Generates high-quality stain-normalized histopathological images [26]. The U-net architecture consists of an encoder and decoder, the encoder down samples the input image to extract hierarchical feature representation, and the decoder reconstructs the image with preserved spatial details. The downsampling procedure integrates convolutional layers, in-stance normalization, and LeakyReLU activation to ensure stable training and enhance feature extraction. The upsampling layers use transposed convolutions to refine the reconstructed images. A Tanh activation function is applied at the final output layer, which guarantees that the generated images have pixel intensities. By preserving both the spatial distribution of tissue structures and the morphological characteristics of cells, the generator effectively learns to map histopathological images into the stain-normalization domain by leveraging this structure [27].

The discriminator evaluates whether the given image is real or generated by a U-net-based generator, and it follows a PatchGAN architecture. The discriminator is performed at the patch level and is focused on the finer details of the tissue regions. By the local receptive field approach, the discriminator ability is increased. It consists of multiple convolutional layers with instance normalization and LeakyReLU activation, which reduces spatial resolution and preserves essential textural details. The indication of each patch being real or, synthetically, the final layer has a probability map. The generator produces high-quality stain-normalized images leveraging PatchGAN.

3.2.2 Perceptual Loss:

To enhance the semantic consistency between the original and stain-normalized images, we use perceptual loss. From a pre-trained deep neural network, perceptual loss evaluates images based on feature representations extracted. L1 or L2 loss focuses on the differences in the intensity of the pixels. For medical image analysis, this method enables the model to capture structural characteristics. To extract feature maps from intermediate layers, we use a VGG16 network, a pre-trained model. This evaluation evaluates the similarity between real and generated images as these feature maps represent high-level hierarchical structures.

$$L_{\text{perceptual}} = \sum_i \| \phi_i(x) - \phi_i(G(x)) \|_2^2 \quad (1)$$

where, $\phi_i(x)$ represents the feature maps extracted from the i-th layer. They use multiple layers to capture both low and high-level structural patterns, as they reserve diagnostic information from normalized images. This prevents the generator from producing smooth images by merging with other loss functions.

3.2.3 Adversarial loss:

The primary objective of adversarial loss function is to produce a high quality stain normalized image in the GAN training process. The discriminator is trained to increase the difference, and the generator is trained to decrease the similarity between real and synthetic images. For adversarial loss, we use BCE with LogitsLoss, which stabilizes learning and prevents degrading gradients. A soft label approach is used assigning 1 for generated images and 0 for fake images to enhance the generator.

It trains the generator to produce images different from real histopathology images guided by adversarial loss. Based on the interactions, the loss is formulated between the generator and PatchGAN.

$$L_{\text{adv}} = \mathrm{E}_{x\sim P_{\text{data}}}[\log D(x)] + \mathrm{E}_{x\sim P_{\text{gen}}}[\log(1-D(G(x)))] \quad (2)$$

where, $D(x)$ is the real image discriminator's prediction, $D(G(x))$ is the generator's prediction. The adverse loss function is used to improve the generator to produce a high-quality normalized image.

3.2.4 Pattern-Preserving Loss:

The structural integrity of histopathological images is not compromised by stain normalization, so we integrate loss-preserving patterns. It enforces similarity between the original and normalized images to maintain morphological and textual details as this loss encourages the generator. To penalize large deviations between input and generated images, we use L1 loss that ensures smooth and stable outputs. The comparison of high-level feature representation is made instead of pixel-wise differences, as we employ a VGG-16 network. Critical histopathological patterns, such as cellular structures and tissue boundaries, allow our model to focus on preservation. We employ pattern preserving loss during stain normalization to ensure that the tissue structure remains intact. This process minimizes the similarities between the original and generated images and maintains morphological characteristics. The L1 norm between the pixel-wise values:

$$L_{\text{pp}} = \| x - G(x) \|_1 \quad (3)$$

The stain normalization does not affect diagnostic accuracy because our proposed work inhibits over-smoothing or loss of histopathological details by implementing pattern-preserving loss. To maintain sharp boundaries between different tissue, this loss is used and it preserves fine-grained details.

3.2.5 Temporal-self Distillation loss:

Due to the unstable nature of adversarial learning, GAN training suffers from insecurity. The regularization of the generator's output is done by this loss function, which executes regularization between various training iterations. This function uses the stable teacher model exponential moving average. With this training the loss of L1 is compared with the output generated by the ema model for purposes of analysis. Improves the overall strength of federated learning, and mode fall-over is eliminated. There are some challenges such as model divergence and instability, so we use this loss function, which stabilizes the training and applies consistency between the generator's output and the ema of the generator.

$$\omega_E = \lambda_E\, \omega + (1-\lambda_E)\, \omega_E \quad (4)$$

λ_E controls the update rate of the E weights. The self-distillation is calculated as:

$$L_{\text{tsd}} = \| G_E(x) - G(x) \|_1 \quad (5)$$

The model updates from multiple clients and introduces noise in the training process. The generator will be stable and maintain consistent outputs.

3.2.6 Overall loss:

We add all the weight of adversarial loss, perceptual loss, pattern-preserving loss, and temporal self-distillation loss.

$$L_{\text{total}} = L_{\text{al}} + \gamma_1 L_{\text{pl}} + \gamma_2 L_{\text{ppl}} + \gamma_3 L_{\text{tsd}} \quad (6)$$

$\gamma 1$, $\gamma 2$, $\gamma 3$ equipose different loss functions and achieve stain normalization across medical datasets and preserves the privacy of data.

3.3 GRAPH CONSTRUCTION

A tissue graph representation is constructed to model spatial and morphological relationships between different tissue regions as it captures the topological organization of the tissue structures[28],[29]. We converted histopathological images into structured graphs despite processing high-resolution images directly because they are computationally expensive. It has good feature extraction, improved tissue structures, and breast cancer subtype classification in this graph-based approach.

3.3.1 Superpixel-based Tissue Segmentation:

Segmenting the histopathology images into meaningful tissue regions is the first step in graph construction. For segmentation, we use the Simple Linear Iterative Clustering(SLIC) [30] algorithm, which is an unsupervised segmentation technique. Homogeneous regions are partitioned over tissue regions according to color, texture, and spatial proximity. Each region in the tissue graph represents the biological structures such as stroma, epithelium, and necrotic tissue, and this superpixel segmentation ensures it. Similar superpixel values are merged with spatial and morphological features into distinct tissue regions when the image is segmented into N superpixels. We point to a centroid in each tissue region that is a graph node. Each node has its own significant structural and functional tissue features.

3.3.2 Feature Extraction:

To extract the feature embeddings, we use a pre-trained ResNet34 model. It extracts deep features and represents histopathological characteristics. The node on the tissue graph is assigned a representation of the characteristic, hiKF, where F is the dimension of the characteristic. For downstream classification tasks, node embeddings are crucial, as they provide discriminative information about cancer subtypes based on the tissue microenvironment.

3.3.3 Graph Construction using Spatial Connectivity:

In the tissue regions, E represents the edges, and V captures spatial interactions between the tissue regions. Based on spatial adjacency and biological relevance, the edges are made. The region Adjacency Graph (RAG) [31] is constructed if the corresponding tissue regions are adjacent where the edge $e(u,v) \in$ E is added between two nodes u and v. An edge $e(u,v)$ is added between two nodes u, v when their represented tissue regionsare adjacent according to the region adjacency graph. The topology of the tissue graph is indicated by a binary adjacency matrix $A \in \mathrm{R}_{N\times N}$, where $A_{u,v} = 1$ if two nodes u,v are connected. Whenever two nodes u and v have adjacent tissue regions according to the region adjacency graph, an edge $e(u,v)$ indicates a learnable embedding function that maps different degrees to distinct representations. Thus, the connectivity embedding (CE) is added to the node features at every transformer layer is added between them. The topology of the tissue graph is defined by a binary adjacency matrix, where $A(u,v) = 1$ means that the two nodes u and v are connected. Finally, the tissue graph of a pathology image is constructed as $T_G(V, E, K)$.

3.4 CONNECTIVITY AWARE GRAPH TRANSFORMER

The idea of the Connectivity-Aware Graph Transformer (CGT) is to improve the representation of tissue graphs by integrating spatial connectivity and long-range dependencies between tissue regions. However, while CGT employs global attention mechanisms, the structure of the histopathology remains unchanged. Essentially, CGT tries to improve the classification of breast cancer subtypes by studying the complex interactions in the microenvironment of a tumor through message passing, Unlike traditional message-passing graph Neural Networks, which base their operations on localized neighborhood aggregation. The CGT model incorporates a Transformer encoder framework, where every graph node (i.e., a tissue region) attends to all the other nodes in the graph to understand both local and global spatial dependencies. It consists of a number of Graph Transformer Layers (GTLs), each of which includes multi-head self-attention (MHA) mechanisms and position-wise feed-forward networks (FFNs). CGT takes input from the tissue graph (*G*), constructed from histopathology images, where the nodes (*V*) represent the tissue regions and the edges (*E*) encode their spatial connectivity. For a specific node v contained in the tissue graph, there are update equations which the Graph Transformer Layer uses for its working.

$$k'(\ell) = M(L(k(\ell-1))) + k(\ell-1) \tag{7}$$

$$k(\ell) = F(L(k'(\ell))) + k'(\ell) \tag{8}$$

where *L* is the layer normalization function, *M* is the multihead attention, *F* represents feed-forward network, *k* is the input of GTL. Such that $k(\ell)$ isn't merely the node features at the ℓ-th GTL, but of course there is also *LN* for layer normalization and *MHA* for multi-head self-attention, which allows nodes to aggregate information regarding each other over the whole graph.

3.4.1 Connectivity Aggregation:

Connectivity embedding for aggregating the local connectivity is different from the GNNs standard Transformers, considering all nodes of the graph as completely connected. It designedly connects local connectivity to tissue by encoding learnable connectivity embeddings (CEs). The degree centrality of a node gives an importance score for that particular node regarding connectivity of the tissue region in the histopathology image. This is defined as:

$$ce_i^{(0)} = n(\mathrm{Deg}(v_i)) \tag{9}$$

where Deg(*v*) denotes the degree of node *v* , while $g(\cdot)$

$$k_i^{(0)} = k_i^{(0)} + \lambda ce_i \tag{10}$$

where, λ is the scaling factor that weighs the contribution of original node features against connectivity embeddings. This condition ensures that the model retains the inherent topology of the graph and does not distort the relationship between tissues based on the self-attention mechanism. There's also the Local Connectivity Aggregate (LCA), which further enhances local connectivity by updating the node connectivity embeddings in each layer.

$$ce_i^{(\ell)} = f_{ce}(ce_i^{(\ell-1)}, ce_j^{(\ell-1)}), \quad \forall j \in N(i) \tag{11}$$

where, $N(i)$ denotes the neighborhood of node *i*, and $fc_e()$ is an aggregation function that updates connectivity embeddings depending on adjacent nodes.

3.4.2 Self-Attention:

Long-range dependencies in spatial proximity information modeling are performed with such introduced connectivity bias in self-attention computation. Weights of attention will be biased towards nodes that are spatially closer in the tissue graph, very much like biological intercellular signaling in a cancerous tissue environment. The connectivity bias is calculated as:

$$\phi(v_i, v_j) = \| q_i - q_j \|_2^2 \tag{12}$$

where q_i and q_j are the spatial coordinates of nodes *i* and *j* respectively. The self-attention mechanism modifies as follows:

$$B_{ij} = \frac{(k_i Y_P)(k_j Y_R)^{\cdot}}{\sqrt{e}} + G\phi(v_i, v_j) \tag{13}$$

$$\text{CB-Attn}(K_{ij}) = \text{softmax}(B_{ij}) k_j Y_R \tag{14}$$

The projection matrices for queries, keys, and values are Y_P , Y_Q, and Y_R, respectively, while C is a learnable parameter that scales the connectivity bias. This makes it possible for CGT to give emphasis to tissues that are nearer while still being able to consider the macrostructure relationships.

4. EXPERIMENTAL SETUP

4.1 DATASETS

For a proper evaluation of the proposed framework, three of the most widely used histopathological datasets were used, namely, BRACS, CRC-VAL-HE-7K, and NCT-CRCHE-100K. These datasets have different staining protocols, tissue architectures, and cancer subtypes, therefore ensuring the robustness of the model in real-life clinical scenarios.

4.1.1 BRACS Dataset [4]:

The BRACS is a large-scale breast cancer histopathology dataset made of 4,391 regions of interest (RoIs) extracted from 325 whole-slide images (WSIs) stained via Hematoxylin and Eosin(H&E). Collected from 151 patients, the dataset was annotated on seven categories by expert pathologists, evil to good. The dataset was scanned and digitized on the high-resolution figure-40× (the Aperio AT2) with a resolution of 0.25 µm per pixel. Thus, allowing for a balanced account and clinically relevant evaluation on the deep learning models. The classes of BRACS are:

- Normal,
- Benign,
- Usual ductal hyperplasia (UDH),
- Atypical ductal hyperplasia (ADH),
- Flat epithelial atypia (FEA),
- Ductal carcinoma in situ (DCIS),

4.1.2 Invasive Carcinoma:

At the ROI level, the dataset is split into training, testing, and validation with a split ratio of 70%,15%, and 15%. ADH and FEA are two difficult diagnostic categories that frequently provide challenges in clinical settings because of their propensity to

evolve into cancer. BRACS encompasses the entire histopathological spectrum of breast cancer. It is a reliable baseline for assessing the effectiveness of graph-based models because of its size and diversity.

4.1.3 CRC-VAL-HE-7K dataset:

The collection contains 7180 high-resolution images of colorectal histopathology annotated into nine different tissue types like tumor epithelium, adipose, lymphocytes, stroma, necrosis, and others, as its name implies[32],[33]. The dataset contains significant staining artifacts, making it an important resource for evaluating the stain normalization capacity of deep learning models. The collection of heterogeneous tissues ensures that the model has to be trained on complex tissue structures and thus prepares it for use in downstream classification and segmentation tasks. It consists of 9 classes:

- Adipose (ADI),
- Background (BACK),
- Debris (DEB),
- Lympocytes (LYM),
- Mucus (MUC),
- Muscle (MUS),
- Normal (NORM),
- Stroma (STR),
- Tumor (TUM)

4.1.4 NCT-CRC-HE-100K:

This is a dataset that consists of 100,000 non-overlapping image patches from (H&E)-stained colorectal cancer tissues, all taken at a 40× magnification. Nine different tissue categories were assigned to the image patches, each capturing histopathological structures in different but balanced proportions. This dataset is likely to help feed the big models of deep learning and is very well known for examining the adaptation of models to variation in staining-to-stain changes since it combines many, many high-resolution image patches having varying staining. This has been benchmarked for applications in research on cancer subtype classification and stain normalization. Thus, it forms a very critical part of our experimental evaluation. It also contains the same class as CRC-VAL-HE-7K.

4.2 EVALUATION MEASURES

SSIM is an effective measure to evaluate the quality of images as perceived by an observer. Unlike older metrics, such as Mean Squared Error (MSE), which treat the input as an array of numbers, the SSIM metric deals with human visual perception and is related to how we observe differences in images. The range of SSIM varies from -1 to +1, with the value of 1 depicting perfect similarity. This is useful for image compression, denoising, and restoration.

FSIM mainly relies on image features and does not treat images as just a series of pixels [34]. Its quality assessment methodologies are based on phase congruency and gradient magnitude. FSIM values lie between 0 and 1, with 1 for identical images. Useful for imparting enhancement and restoration to images, especially topical where structural features are of prime interest.

Table.1. Comparison of models with Proposed Work

Method	Precision	Recall	F1-Score	Accuracy
ResNet50	85.12	77.89	75.6	77.78
Swin Transformer	88.2	87.5	85.8	80.95
Proposed	88.9	85.9	85.9	87.22

Accuracy is a naive measure that tells you what percentage of the model's predictions were correct overall. It could be easily misleading when it comes to imbalanced datasets. Scores lying between 0% and 100%, an imbalanced dataset would score high on accuracy, though all the wrong predictions would be for the minority class.

Table.2. Evaluation Results across Datasets

Dataset	F1-score	Precision	Recall	Accuracy
CRC-VAL-HE-7K	85.9	88.9	85.9	87.22
NCT-CRC-HE-100K	84.9	84.9	89.0	85.4

The model training is optimized to fully utilize GPU capabilities; this has significantly facilitated faster convergence and large-scale batch processing. The assigned computation platform is designed in such a way that it can process high resolution histopathology images and large functional graphs without running into memory bottlenecks.

$$Accuracy = \frac{TP + TN}{TP + TN + FP + FN} \tag{15}$$

Precision tells us how good the positive predictions are. It matters the most when the cost of false positives is high. The precision value ranges from 0 to 1, higher meaning better performance. This is again very much useful in medical diagnosis, spam detection, and other areas with substantial consequences from false positives.

$$\text{Precision} = \frac{TP}{TP + FP} \tag{16}$$

Recall quantifies the ability of a model to detect all the relevant instances. It becomes very important in scenarios where missing a positive case is critical. Recall also varies from 0 to 1. Important in disease detection, fraud detection, and any context where false negatives incur high costs.

$$\text{Recall} = \frac{TP}{TP + FN} \tag{17}$$

F1-score is a measure for a test's accuracy that considers both the precision and the recall scores of that test in computing the overall score. Most important, it can be used for highly imbalanced datasets where one class may be important as compared to the other. Ranges from 0 to 1, where the value 1 indicates perfect precision and recall. Used in binary classification problems most commonly in the area of medical diagnosis, fraud detection, and information retrieval.

$$\text{F1-score} = \frac{2\,\text{Precision} \cdot \text{Recall}}{\text{Precision} + \text{Recall}} \tag{18}$$

4.3 IMPLEMENTATION DETAILS

All hyper-parameters used in training and testing to an arbitrary configuration were implemented using PyTorch [35] and

the Deep Graph Library (DGL) [36]. The training was performed for 100 epochs with the Adam optimizer [37], having a base learning rate of 1e-3 and a batch size of 4. The use of a weight decay of 1e-3 was enforced for preventing overfitting. The dimension of the node feature is fixed to 514 to balance model complexity against computational efficiency. The sum function was finally selected for local connectivity aggregation, as it offered better performance than the other contenders in this space: mean, max, and min. All experimental runs were done on an NVIDIA GeForce RTX 3090 GPU with 36 GB memory.

5. EXPERIMENTAL RESULTS

5.1 COMPARISON BETWEEN PROPOSED AND TRADITIONAL METHODS

We first demonstrate the work without stain normalization with the BRCACS dataset for breast cancer classification. Then, the stain normalization GAN work is proposed for better classification accuracy on CRC-VAL-HE-7K and NCT-CRCHE-100K.

Since the dataset is large we have also calculated the F1-score, Precision, Recall for performance evaluation. To predict the classification, we calculated accuracy. We classify it on two datasets where their evaluation results are reported in You can refer to the table as Table.2 and it is visualized as graphs in Fig.3. The CGT model is compared with other models for test set [38].

The other two network architectures used are, ResNet50 and Swin Transformer for classification. But our proposed achieved better classification accuracy other than that. The model comparison is calculated with evaluation metrics and comparison is given in Table.1.

For image generation using stain normalization GAN, we calculated the average generator and discriminator loss, and SSIM, FSIM score for each class in the dataset. And it is also differentiated in colors in Fig.3.

5.2 ABLATION STUDY

We perform ablations on the pattern preserving loss, temporal self-distillation, etc. Here, the pattern preserving loss is such a loss in performance as a result of an absence that it is more than that of other components. The ablation provides empirical evidence for the efficacy of different components. Thus, we have designed a pattern preserving loss to tackle the problem of preserving the structural components. Ablations can then be carried out first to test whether pattern preserving loss has some significance on the preservation of semantic structure information, the degree of which can be evaluated through the SSIM established between an original image and the normalized image.

Our connectivity attributes include CE and CB. Both were shown in the ablation study before, where both these attributes had rather considerable effects on the performance of the model with respect to breast cancer classification. CE incorporates graph topology adding learnable connectivity embedding to node features, which is initialized by graph node degree. Further, CB aggregates spatial distance between two nodes by mapping node pair distance to learnable vector while computing self-attention among nodes. Noteworthy is that our CE and CB are tied to the structure of the input graph, e.g., the number and degree of nodes, and denseness or sparseness of the graph.

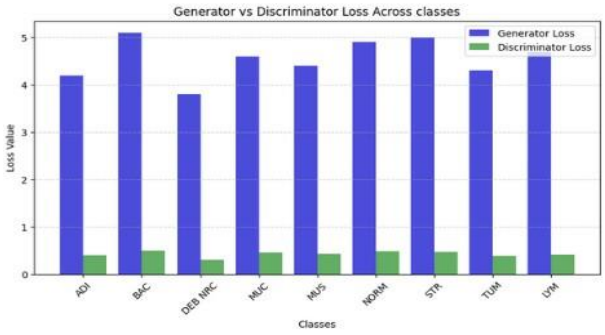

(a) Generator Discriminator Loss

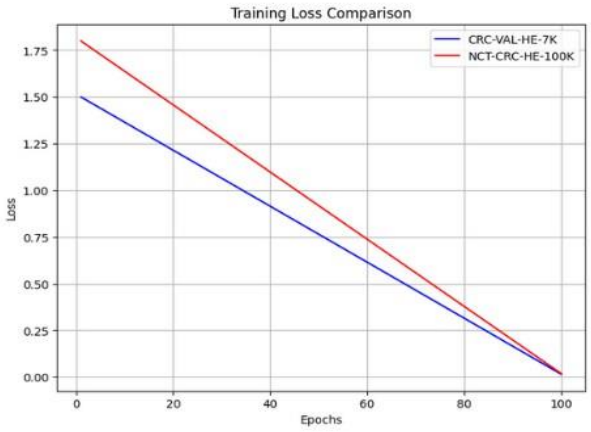

(b) Training Loss over epochs

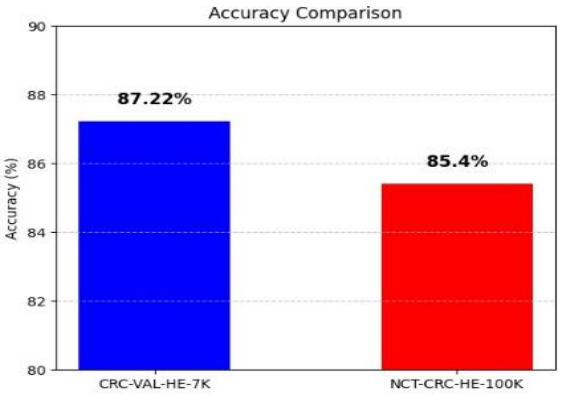

(c) Accuracy over epochs

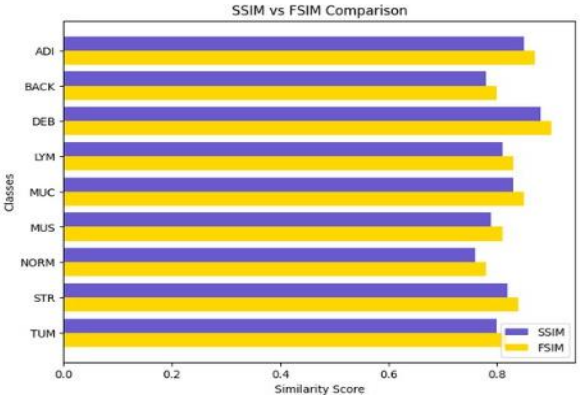

(d) SSIM vs. FSIM Score

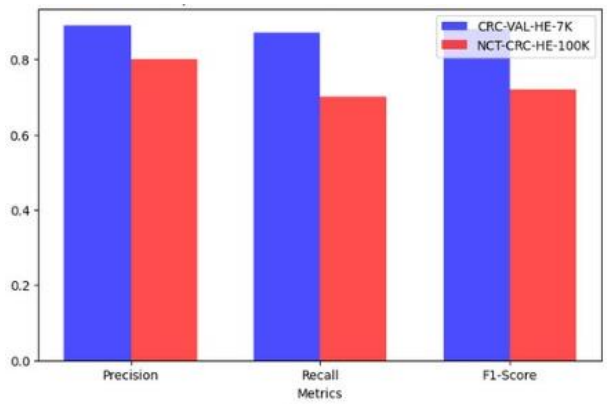

(e) Precision, Recall and F1-Score

Fig.3. Evaluation measures of our proposed system

6. CONCLUSION

The CGT framework for classifying breast cancer using stain-normalized histopathology pictures with tissue graph representations. The methodology used GAN-based stain normalization, graph based histopathological representation learning, and self-attention mechanisms to boost the classification performance. This as CGT model has been able to capture spatial views of tissue regions improving accuracy in classification as compared to CNNs and message-passing GNNs.

Experimentations with the BRACS, CRC-VAL-HE-7K, and NCT-CRC-HE-100K datasets proved our approach very effective in achieving good results. The improvement on the robustness of a model through staining artifacts brought about by the stain normalization module, coupled with the graph-based representation learning, enabled better understanding of structural analysis of tissues.

Apart from this GCNs, transformer-based GNNs, vision transformer models form comparisons with state-of-the art message passing. Our method holds promise for enhanced understanding breast cancer classification while making the approach explainable through self-supervised learning, hierarchical tissue representations, and transformer-based GNNs. In sum, the framework establishes a new benchmark in the analysis of histopathological images by bringing together deep learning-based stain normalization with graph-based cancer diagnosis.

Some of the areas in which improvements could eventually be made towards making the CGT framework more efficient and relevant for application to the real clinical environment have been identified despite its having already shown stateof-the-art performance with respect to stain normalization and histopathological classification. For example, Integrating next-gen multi-model medical data genomics profiles, clinical reports, radiological scan, for a better in-depth insight about cancer progression, will try to embrace WSI metadata and molecular biomarkers towards better diagnosis within future research.

An explainable AI (XAI) module to visualize attention maps, tissue interactions, and classification reasoning will promote model interpretation. This will go a long way toward helping pathologists understand model predictions and thereby increase trust in AI-based diagnostics. Improving generalizability of the model across different multicenter histopathology datasets by improving stain normalization using unsupervised domain adaptation and contrastive learning techniques.

REFERENCES

[1] K. Wang, F. Zheng, L. Cheng, H.N. Dai, Q. Dou and J. Qin, "Breast Cancer Classification from Digital Pathology Images via Connectivity-Aware Graph Transformer", *IEEE Transactions on Medical Imaging*, Vol. 43, No. 8, pp. 2854-2865, 2024.

[2] Y. Shen, A. Sowmya, Y. Luo, X. Liang, D. Shen and J. Ke, "A Federated Learning System for Histopathology Image Analysis with an Orchestral Stain-Normalization GAN", *IEEE Transactions on Medical Imaging*, Vol. 42, No. 7, pp. 1969-1981, 2023.

[3] F. Ciompi, "The Importance of Stain Normalization in Colorectal Tissue Classification with Convolutional Networks", *Proceedings of International Symposium on Biomedical Imaging*, pp. 160-163, 2017.

[4] M. Sureka, A. Patil, D. Anand and A. Sethi, "Visualization for Histopathology Images using Graph Convolutional Neural Networks", *Proceedings of International Conference on Bioinformatics and Bioengineering*, pp. 331-335, 2020.

[5] O. Ronneberger, P. Fischer and T. Brox, "U-Net: Convolutional Networks for Biomedical Image Segmentation", *Proceedings of International Conference on Medical Image Computing and Computer-Assisted Intervention*, pp. 234-241, 2015.

[6] M. Sheller, "Federated Learning in Medicine: Facilitating Multi-Institutional Collaborations without Sharing Patient Data", *Scientific Reports*, Vol. 10, No. 1, pp. 1-12, 2020.

[7] D. Onder, S. Zengin and S. Sarioglu, "A Review on Color Normalization and Color Deconvolution Methods in Histopathology", *Applied Immunohistochemistry Molecular Morphology*, Vol. 22, No. 10, pp. 713-719, 2014.

[8] J. Ke, Y. Shen and Y. Lu, "Style Normalization in Histology with Federated Learning", *Proceedings of International Symposium on Biomedical Imaging*, pp. 953-956, 2021.

[9] Vahadane, "Structure-Preserving Color Normalization and Sparse Stain Separation for Histological Images", *IEEE Transactions on Medical Imaging*, Vol. 35, No. 8, pp. 1962-1971, 2016.

[10] M.T. Shaban, C. Baur, N. Navab and S. Albarqouni, "Staingan: Stain Style Transfer for Digital Histological Images", *Proceedings of International Symposium on Biomedical Imaging*, pp. 953-956, 2019.

[11] M.Y. Lu, "Federated Learning for Computational Pathology on Gigapixel Whole Slide Images", *Medical Image Analysis*, Vol. 76, pp. 1-9, 2022.

[12] Q. Liu, C. Chen, J. Qin, Q. Dou and P.A. Heng, "FedDG: Federated Domain Generalization on Medical Image Segmentation via Episodic Learning in Continuous Frequency Space", *Proceedings of International Conference on Computer Vision and Pattern Recognition*, pp. 1013-1023, 2021.

[13] J. Ke, "Multiple-Datasets and Multiple-Label based Color Normalization in Histopathology with cGAN" *Proceedings of International Conference on SPIE*, Vol. 11603, pp. 1-7, 2021.

[14] M. Macenko, "A Method for Normalizing Histology Slides for Quantitative Analysis", *Proceedings of International Symposium on Biomedical Imaging*, pp. 1107-1110, 2009.

[15] P. Salehi and A. Chalechale, "Pix2Pix-based Stain-to-Stain Translation: A Solution for Robust Stain Normalization in Histopathology Images Analysis", *Proceedings of International Conference on Machine Vision and Image Processing*, pp. 1-7, 2020.

[16] H. Nazki, O. Arandjelovic, I. Um and D. Harrison, "Multi-PathGAN: Structure Preserving Stain Normalization using Unsupervised Multi-Domain Adversarial Network with Perception Loss", *Proceedings of International Conference on Computer Vision and Pattern Recognition*, pp. 1-13, 2022.

[17] M. Macenko, "A Method for Normalizing Histology Slides for Quantitative Analysis", *Proceedings of International Symposium on Biomedical Imaging*, pp. 1107-1110, 2009.

[18] L. Studer, J. Wallau, H. Dawson, I. Zlobec and A. Fischer, "Classification of Intestinal Gland Cell-Graphs using Graph Neural Networks", *Proceedings of International Conference on Pattern Recognition*, pp. 3636-3643, 2021.

[19] P. Pati, G. Jaume, L.A. Fernandes, A. Foncubierta-Rodrıguez, F. Feroce,M. Anniciello, G. Scognamiglio, N. Brancati, D. Riccio and M.D. Bonito, "Hact-Net: A Hierarchical Cell-to-Tissue Graph Neural Network for Histopathological Image Classification", *Uncertainty for Safe Utilization of Machine Learning in Medical Imaging and Graphs in Biomedical Image Analysis*, pp. 208-219, 2020.

[20] Aygunes, S. Aksoy, R.G. Cinbis, K. Kosemehmetoglu, S. Onder and A. Uner, "Graph Convolutional Networks for Region of Interest Classification in Breast Histopathology", *International Society for Optics and Photonics*, Vol. 11320, pp. 1-7, 2020.

[21] J. Ke, Y. Shen, X. Liang and D. Shen, "Contrastive Learning based Stain Normalization Across Multiple Tumor Histopathology", *Proceedings of International Conference on Medical Image Computing and Computer Assisted Intervention*, pp. 571-580, 2021.

[22] V.P. Dwivedi and X. Bresson, "A Generalization of Transformer Networks to Graphs", *Proceedings of International Conference on Machine Learning*, pp. 1-8, 2020.

[23] D. Kreuzer, D. Beaini, W. Hamilton, V. Letourneau and P. Tossou, "Rethinking Graph Transformers with Spectral Attention", *Advances in Neural Information Processing Systems*, Vol. 34, pp. 21618-21629, 2021.

[24] X. Wang, S. Yang, J. Zhang, M. Wang, J. Zhang, J. Huang, W. Yang and X. Han, "Transpath: Transformer-based Self-Supervised Learning for Histopathological Image Classification", *Proceedings of International Conference on Medical Image Computing and Computer Assisted Intervention*, pp. 186-195, 2021.

[25] W. Hu, B. Liu, J. Gomes, M. Zitnik, P. Liang, V. Pande and J. Leskovec, "Strategies for Pre-training Graph Neural Networks", *Proceedings of International Conference on Learning Representations*, pp. 1-22, 2020.

[26] Anghel, "A High-Performance System for Robust Stain Normalization of Whole-Slide Images in Histopathology", *Frontiers in Medicine*, Vol. 6, pp. 1-8, 2019.

[27] D. Tellez, "Quantifying the Effects of Data Augmentation and Stain Color Normalization in Convolutional Neural Networks for Computational Pathology", *Medical Image Analysis*, Vol. 58, pp. 1-8, 2019.

[28] D. Anand, S. Gadiya and A. Sethi, "Histographs: Graphs in Histopathology", *Proceedings of International Conference on Medical* Imaging, Vol. 11320, pp. 150-155, 2020.

[29] P. Pati, G. Jaume, A. Foncubierta-Rodrıguez, F. Feroce, A.M. Anniciello, G. Scognamiglio, N. Brancati, M. Fiche, E. Dubruc and D. Riccio, "Hierarchical Graph Representations in Digital Pathology", *Medical Image Analysis*, Vol. 75, pp. 1-7, 2022.

[30] R. Achanta, A. Shaji, K. Smith, A. Lucchi, P. Fua and S. Susstrunk, "Slic Superpixels Compared to State-of-the-Art Superpixel Methods", *IEEE Transactions on Pattern Analysis and Machine Intelligence*, Vol. 34, No. 11, pp. 2274-2282, 2012.

[31] F.K. Potjer, "Region Adjacency Graphs and Connected Morphological Operators", *Mathematical Morphology and its Applications to Image and Signal Processing*, pp. 111-118, 1996.

[32] Marmol, C. Sanchez-de-Diego, A.P. Dieste, E. Cerrada and M.R. Yoldi, "Colorectal Carcinoma: A General Overview and Future Perspectives in Colorectal Cancer", *International Journal of Molecular Sciences*, Vol. 18, No. 1, pp. 1-7, 2017.

[33] Kather, "Predicting Survival from Colorectal Cancer Histology Slides using Deep Learning: A Retrospective Multicenter Study", *PLOS Medicine*, Vol. 16, No. 1, pp. 2-9, 2019.

[34] Zhang, L. Zhang, X. Mou and D. Zhang, "FSIM: A Feature Similarity Index for Image Quality Assessment", *IEEE Transactions on Image Processing*, Vol. 20, No. 8, pp. 2378-2386, 2011.

[35] Paszke, S. Gross, F. Massa, A. Lerer, J. Bradbury, G. Chanan, T. Killeen, Z. Lin, N. Gimelshein and L. Antiga, "Pytorch: An Imperative Style, High-Performance Deep Learning Library", *Advances in Neural Information Processing Systems*, Vol. 32, pp. 1-12, 2019.

[36] Y. Wang, "Deep Graph Library: Towards Efficient and Scalable Deep Learning on Graphs", *ICLR Workshop on Representation Learning on Graphs and Manifolds*, pp. 1-19, 2019.

[37] D.P. Kingma and J. Ba, "Adam: A Method for Stochastic Optimization", *Proceedings of International Conference on Learning Representations*, pp. 1-13, 2014.

[38] S.S. Chennamsetty, M. Safwan and V. Alex, "Classification of Breast Cancer Histology Image using Ensemble of Pre-Trained Neural Networks", *Proceedings of International Conference Image Analysis and Recognition*, pp. 804-811, 2018.